Electron-Ion Coincidence Spectroscopy on Atomic Barium in the Excitation Range of the 4*d* Giant Resonance

S. Baier, G. Gottschalk, T. Kerkau, T. Luhmann, M. Martins, M. Richter, G. Snell, and P. Zimmermann

Institut für Strahlungs- und Kernphysik, Technical University, D-10623 Berlin, Germany

(Received 30 August 1993)

For the first time a free metal atom has been investigated by analyzed electron-ion coincidence spectroscopy after inner-shell excitation with synchrotron radiation. Probabilities of the decay from different Ba^+ inner-hole states ($4d^{-1}$, $5s^{-1}$, $5p^{-1}$) to higher charged ions (Ba^{2+}, Ba^{3+}, Ba^{4+}) have been determined, which allows a direct link between electron and ion spectroscopy results. Comparison between the different data sets and Hartree-Fock calculations for N_{45} Auger transitions yields new knowledge about direct double ionization processes, e.g., their dominance on $4d^{-1}$ Auger decay.

PACS numbers: 32.80.Fb, 32.80.Hd

Spectroscopy on free atoms photoexcited in the energy range of the vacuum ultraviolet VUV has been established for many years to be well suited for the investigation of many-body effects. In most cases radiationless decay of the highly excited states dominates by far and leads to multiply charged ions in the final states by a series of many-electron correlation processes. In this context the discussion is now more and more focused on the different mechanisms of multiple ionization, i.e., multistep ionization and direct multiple ionization (see, e.g., Refs. [1–3] and references therein). Electron-ion coincidence spectroscopy is an ideal tool to study these decay cascades since this experimental method relates information about the first steps of a decay obtained by electron spectroscopy to information about the final states obtained by ion spectroscopy.

The experimental setup is shown in Fig. 1. Monochromatized synchrotron radiation from BESSY crosses a beam of free Ba atoms. Photofragments are analyzed by an electrostatic electron spectrometer and a time-of-flight ion spectrometer. A photoionization process is investigated by setting first the electron analyzer energy to the kinetic energy of the corresponding photoelectron. Then electrostatic ion extraction pulses are triggered by the electron signals and the time-of-flight spectrum of coincident ions is measured.

The 4*d* giant resonance of atomic Ba ([Kr] $4d^{10}5s^25p^66s^2$) is a prominent example for strong many-electron effects (see, e.g., Refs. [4–7] and references therein). In Fig. 2 two photoelectron spectra of Ba are displayed which were taken in the photon energy range of the resonance and demonstrate the manyfoldness of the processes. Numerous discrete photoelectron lines can be observed due to photoionization of the 6*s*, 5*p*, 5*s*, and 4*d* shells. Besides them a number of Auger lines arise ($N_{45}O_{23}O_{23}$, $N_{45}O_1V$, $N_{45}O_{23}V$; V stands for valence electron) due to the decay of $4d^{-1}$ hole states. Finally a photoionization background appears at high binding energy. Its intensity varies with photon energy and is correlated with $4d^{-1}\varepsilon f$ photoionization strength. This background has been explained by direct double ionization processes, i.e., direct double photoionization (shakeoff) and/or direct double Auger decay [5,6].

A part of the described photoionization processes has been investigated in the present study by electron-ion coincidence spectroscopy and the corresponding results are summarized in Table I. $6s^{-1}$ photoionization ends up in the Ba^+ ground state (Fig. 3) and no further decay is possible. In contrast $5p^{-1}$ and $5s^{-1}$ hole states are located well above the Ba^{2+} $6s^{-2}$ threshold but also well below the Ba^{3+} limit. The coincidence measurements for

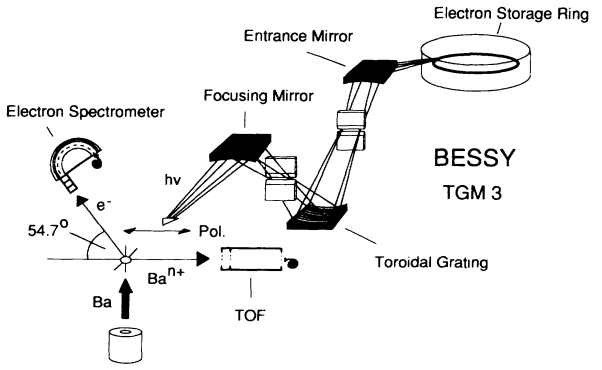

FIG. 1. Experimental setup.

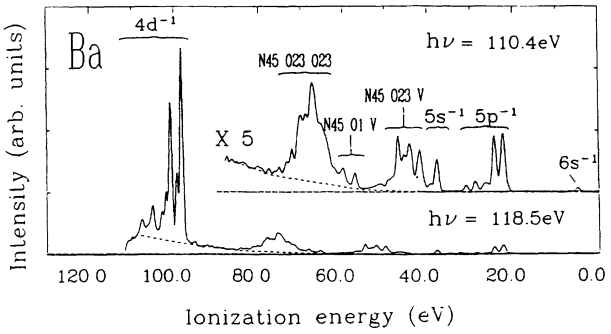

FIG. 2. Photoelectron spectra of atomic Ba ([Kr] $4d^{10}5s^2$-$5p^66s^2$) taken at 110.4 and 118.5 eV photon energy [5].

0031-9007/94/72(18)/2847(4)$06.00

TABLE I. Electron-ion coincidence results for different hole states of atomic Ba ([Kr] $4d^{10}5s^25p^66s^2$).

Initial state	E_B (eV) (Ref. [5])	Decay probabilities 2+	3+	4+
$5p_{3/2}^{-1}$	22.7	1.00(1)	...	...
$5s^{-1}$	37.9	1.00(1)	...	...
$4d_{5/2}^{-1}$	98.4	0.12(3)	0.86(3)	0.02(2)
$4d_{5/2}^{-1}6s^{-1}4f$	99.5	0.04(2)	0.92(2)	0.04(2)
$4d_{3/2}^{-1}$	101.0	0.17(3)	0.83(3)	0.01(1)
$4d_{5/2}^{-1}6s^{-1}7s$	105.3	0.08(3)	0.87(3)	0.05(3)

these photoionization processes result, indeed, in decay probabilities into Ba^{2+} final states of 100% (Table I). This indicates that fluorescence decay into Ba^+ final states does not play any role within the given error bars.

The $4d^{-1}$ photoionization processes lead to Ba^{2+}, Ba^{3+}, and Ba^{4+} final states but the transition probabilities vary strongly for the different $4d^{-1}$ configurations (Table I). The decay behavior after the $4d_{3/2,5/2}^{-1}$ main processes differs significantly from that of the corresponding processes on Xe [8]: the Ba^+ $4d_{3/2}^{-1}$ hole state couples to a Ba^{3+} final state more weakly than the $4d_{5/2}^{-1}$ counterpart although it is localized at higher binding energy. In this context it might be important that for Ba the first threshold for triple photoionization is far away from the $4d^{-1}$ ionization limits (Fig. 3), whereas the Xe $4d^{-1}$ and Xe^{3+} thresholds overlap.

To get more detailed information about the decay behavior of Ba^+ $4d^{-1}$ hole states the $Ba^+4d^{-1} \rightarrow Ba^{2+}(\varepsilon l)_{Au}N_{45}$ Auger spectrum has been calculated by a Hartree-Fock method with relativistic correction using the Cowan code [9]. Satellite processes are not taken into account. The results are shown in Fig. 4. They are compared to an experimental Auger spectrum which has been obtained using the undispersed white light of the zero order of a toroidal grating monochromator at BESSY. The high background in this spectrum is due to direct photoionization processes. The discrete line structures between 5 and 17 eV have been well investigated and correspond exclusively to O_{23} Auger emission and autoionization of $5p^{-1}nd$ excited states [10,11]. One result of the calculations is that experimental and theoretical N_{45} Auger spectra agree excellently in the higher energy range if for the initial state of the Auger decay configuration mixing between $4d^95s^25p^6$ ($6s^2$,$5d6s$,$5d^2$) configurations is included. To obtain the mixing parameters the preceding $4d^{-1}\varepsilon l$ photoionization process has also been calculated, including here configuration interaction between $6s^2$ and $5d^2$ for the initial state of the photoionization.

The calculated relative strengths for the different Auger processes (Fig. 4) can be used to get information about the charge in the final state of a $4d^{-1}$ photoionization after a complete Auger decay cascade. For that it is

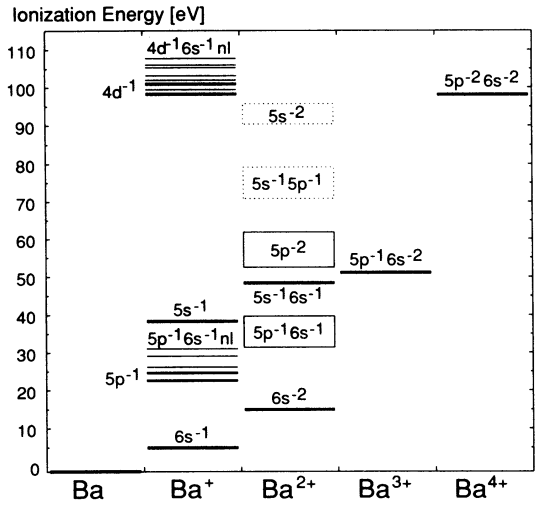

FIG. 3. Energy level diagram of atomic Ba ([Kr] $4d^{10}5s^2$-$5p^66s^2$).

assumed that a Ba^{2+} state, which is reached by a first Auger process after $4d^{-1}$ photoionization, decays further by following Auger transitions into Ba^{3+} or Ba^{4+} final states if it is possible energetically. This assumption seems reliable since, indeed, charge conserving fluorescence has been proved to be negligible in the energy range of the VUV if compared to a competing Auger process as shown for the decay of $4d^{-1}$, $5s^{-1}$, and $5p^{-1}$

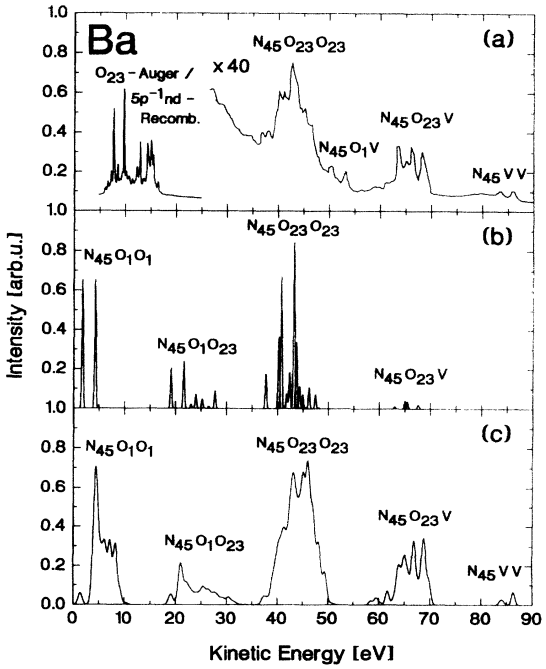

FIG. 4. (a) Experimental and (b),(c) calculated Ba N_{45} Auger spectra [(b), without $6s$-$5d$ mixing; (c), $6s$-$5d$ mixing for $4d^{-1}$ states included].

hole states. However, according to the energy level diagram in Fig. 3, $6s^{-2}$, $5p^{-1}6s^{-1}$, and $5s^{-1}6s^{-1}$ Ba^{2+} states, reached after $N_{45}VV$, $N_{45}O_{23}V$, and $N_{45}O_1V$ Auger transitions, are localized below the Ba^{3+} threshold and therefore lead to Ba^{2+} final states. All other Auger channels should end up in Ba^{3+} or Ba^{4+}.

In Table II the results for decay probabilities into Ba^{n+} final states after $4d^{-1}$ photoionization deduced from the calculations for the Auger transitions are summarized and compared to the corresponding experimental values of Table I. Better agreement is obtained if $6s$-$5d$ mixing is taken into account, whereas decay to Ba^{3+} or Ba^{4+} is overestimated by far if $6s$-$5d$ mixing is neglected. In other words, $6s$-$5d$ mixing results in more Ba^{2+} in the final state. The latter can be explained by the $5d$ wave function collapse: More $5d$ character of the valence electrons implies that they couple more strongly to the $5p^6$ shell which should favor $N_{45}O_{23}V$ Auger transitions $[4d^{-1} \rightarrow 5p^{-1}(6s,5d)^{-1}(\varepsilon l)_{Au}]$ leading to Ba^{2+} in the final state (Fig. 3).

In the photoelectron spectra of Fig. 2 background is also observed which is probably in part due to direct double Auger decay [5,6]. Our analysis of this spectrum and all original data of Ref. [5] confirms that such processes account for $(61 \pm 8)\%$ of the total N_{45} Auger strength since only $(39 \pm 8)\%$ is found in the spectra as clearly perceptible Auger lines and strong $4d^{-1}$ fluorescence decay channels ending up in Ba^+ were not observed. Direct double Auger leads in any case to Ba^{3+} or Ba^{4+} final states and has not been taken into consideration by the performed Hartree-Fock calculations. But although this dominating process is neglected the deduced probabilities for decay to Ba^{n+} agree fairly well with the corresponding experimental data as discussed below (Table II). Two tentative explanations can be given: (a) The coupling mechanism to Ba^{3+} and Ba^{4+} continua (multistep ordinary Auger or direct multiple Auger) does not strongly influence the transition probabilities to Ba^{3+} and Ba^{4+}. (b) The direct double Auger mechanism may also be regarded as a sort of two-step process where energy exchange of the two Auger electrons leads to a continuous electron emission. In any case this implies that a strong part of the calculated $N_{45}OO$ Auger oscillator strength in Fig. 4 is in fact transferred to double Auger continua which is supported by the quite intense $N_{45}O_1$-O_1 and $N_{45}O_1O_{23}$ Auger structures of Figs. 4(b) and 4(c) which are not even only in part but completely vanished in the experimental spectrum.

TABLE II. Probabilities for the decay of $4d_{3/2,5/2}^{-1}$ hole states to Ba^{n+}. a: experiment (Table I); b: theory without $6s$-$5d$ mixing; c: $6s$-$5d$ mixing included for the $4d^{-1}$ ionic states.

Initial state	Decay probabilities					
	a		b		c	
	2+	3+,4+	2+	3+,4+	2+	3+,4+
$4d_{3/2}^{-1}$	0.17(3)	0.83(3)	0.03	0.97	0.21	0.79
$4d_{5/2}^{-1}$	0.12(3)	0.88(3)	0.03	0.97	0.14	0.86

Besides the possibility to investigate Auger decay probabilities electron-ion coincidence spectroscopy also has the more general aspect of a direct link between electron and ion spectroscopy. Table I, which contains the present results of electron-ion coincidence spectroscopy, can be interpreted as a matrix M which couples the cross section vector σ_{PIS} for photoion spectroscopy and the cross section vector σ_{PES} for photoelectron spectroscopy by

$$\sigma_{PIS} = M\sigma_{PES}. \quad (1)$$

The components of the cross section vectors are the partial photoionization cross sections: $\sigma_{PIS} = [\sigma^+(h\nu), \sigma^{2+}(h\nu), \ldots]$, $\sigma_{PES} = [\sigma^{P1}(h\nu), \sigma^{P2}(h\nu), \ldots]$, where Pn denotes the first step of a photoionization process, e.g., $6s^{-1}$, $5p_{1/2}^{-1}$, etc. If the coincidence matrix M is known completely, σ_{PIS} can be calculated from σ_{PES} by formula (1).

Unfortunately the present coincidence matrix of Table I is not complete. But the missing information can be obtained nevertheless. As mentioned before, $6s^{-1}$ photoionization must end up by 100% in a Ba^+ state. All $5p^{-1}$ processes should end up in Ba^{2+} in analogy to the $5p_{1/2}^{-1}$ main process since all corresponding $5p^{-1}6s^{-1}nl$ configurations are localized above the Ba^{2+} threshold but below the Ba^{3+} limit (see Fig. 3). Finally the decay behavior of the missing $4d^{-1}$ satellite processes can be estimated from the results of the investigated processes which show a higher decay probability to Ba^{3+} and Ba^{4+} as do the $4d^{-1}$ main lines (Table I).

With the help of formula (1) using the present coincidence results and electron spectroscopy data [5] the cross section ratio $(\sigma^{3+}+\sigma^{4+})/\sigma^{total}$ has been calculated. The result is displayed in Fig. 5 as a function of photon energy and compared with results of photoion spectroscopy [4]. Above the first $4d^{-1}$ threshold at 98.4 eV agreement is obtained within the error bars. Obviously there is

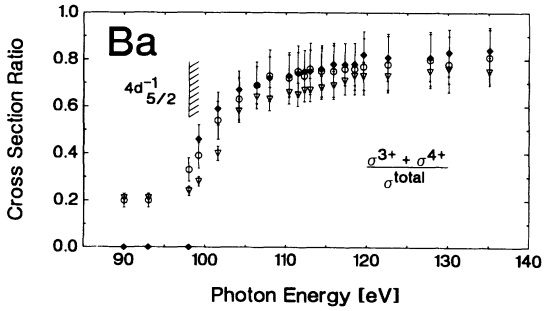

FIG. 5. Cross section ratio $(\sigma^{3+}+\sigma^{4+})/\sigma^{total}$. Filled symbols: deduced from photoelectron spectroscopy data [5] and coincidence results. Open symbols: photoion spectroscopy results (open circles: Ref. [4]). The first $4d^{-1}$ ionization threshold is indicated.

no important photoionization channel missing, which implies that direct double photoionization (shakeoff) seems to be less important in the photon energy range of the $4d^{-1}\varepsilon f$ giant resonance: (1) Shakeoff photoelectrons share the available kinetic energy leading also to unstructured background in photoelectron spectra as does direct double Auger emission. (2) Background has been subtracted in the evaluation of the photoelectron spectroscopy data and therefore intensity due to shakeoff would be missing [5]. (3) Since the background has been observed only at ionization energies above the Ba^{3+} threshold at 51 eV (Figs. 2 and 3) shakeoff processes have to end up in Ba^{3+} or Ba^{4+} final states. (4) Missing shakeoff intensity would then result in the observation of less Ba^{3+} or Ba^{4+} intensity calculated according to formula (1) and in a smaller ionization cross section ratio $(\sigma^{3+}+\sigma^{4+})/\sigma^{\text{total}}$. The data in Fig. 5 show this only below the $4d^{-1}$ thresholds. The observed background in photoelectron spectra taken at photon energies of the giant resonance (Fig. 2) must therefore be related mainly to double Auger processes and not to direct double photoionization.

In conclusion it can be summarized that for different Ba^{+} hole states ($4d^{-1}$, $5s^{-1}$, $5p^{-1}$) probabilities of Auger decay to Ba^{2+},Ba^{3+}, and Ba^{4+} have been determined using an electron-ion coincidence technique.

Comparison with Hartree-Fock calculations shows that the $4d^{-1}$ decay probabilities depend strongly on $6s$-$5d$ mixing of the Ba^{+} $4d^{-1}$ hole states but less on the Auger decay mechanism leading to higher charged ions (Ba^{3+}, Ba^{4+}) which may be tentatively explained by an equivalence of multistep ordinary Auger and direct multiple Auger. Many-body calculations are needed to test this idea.

The coincidence results allow a direct link between photoion spectroscopy and photoelectron spectroscopy. In this context it is found that direct double photoionization seems to be only a weak photoionization channel in the photon energy range of the $4d^{-1}\varepsilon f$ giant resonance. Background in corresponding photoelectron spectra [5,6] is identified to be mainly double Auger emission which accounts for $(61 \pm 8)\%$ of the $4d^{-1}\varepsilon f$ cross section.

The authors thank the BESSY staff for assistance. The financial support of the Bundesministerium für Forschung und Technologie is gratefully appreciated.

[1] G. B. Armen and F. P. Larkins, J. Phys. B **24**, 741 (1991).
[2] M. Ya. Amusia, V. A. Kilin, A. Ehresmann, H. Schmoranzer, and K. H. Schartner, J. Phys. B **26**, 1281 (1993).
[3] I. Lee, R. Wehlitz, U. Becker, and M. Ya. Amusia, J. Phys. B **26**, L41 (1993).
[4] T. Nagata, Y. Itoh, Y. Itikawa, T. Koizumi, T. Matsuo, Y. Sato, E. Shigemasa, A. Yagishita, and M. Yoshino, J. Phys. B **22**, 3865 (1989).
[5] M. Richter, M. Meyer, M. Pahler, T. Prescher, E. v. Raven, B. Sonntag, and H. E. Wetzel, Phys. Rev. A **39**, 5666 (1989); **40**, 7007 (1989); M. Richter, Ph.D. thesis, University of Hamburg [DESY Internal Report No. F41-88/05, Hamburg, 1988 (unpublished)].
[6] J. M. Bizau, D. Cubaynes, P. Gérard, and F. J. Wuilleumier, Phys. Rev. A **40**, 3002 (1989).
[7] V. Radojevic, M. Kutzner, and H. P. Kelly, Phys. Rev. A **40**, 727 (1989).
[8] B. Kämmerling, B. Krässig, and V. Schmidt, J. Phys. B **25**, 3621 (1992).
[9] R. D. Cowan, *The Theory of Atomic Structure and Spectra* (University of California Press, Berkeley, 1981).
[10] D. Rassi and K. J. Ross, J. Phys. B **13**, 4683 (1980).
[11] R. A. Rosenberg, S.-T. Lee, and D. A. Shirley, Phys. Rev. A **21**, 132 (1980).

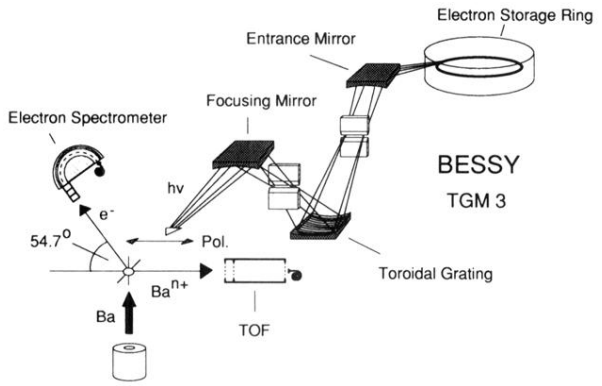

FIG. 1. Experimental setup.